

abilities in transformed HaCaT keratinocytes within 24 h, is of interest to the development of tumor suppressors.

Received: May 21, 2002 [Z19348]

- [1] O. Huber, C. Bierkamp, R. Kemler, *Curr. Opin. Cell Biol.* **1996**, *8*, 685–691.
- [2] Y. Saeki, K. Hazeki, M. Matsumoto, K. Toyoshima, H. Akedo, T. Seya, *Oncol. Rep.* **2000**, *7*, 731–735.
- [3] M. Takeichi, *Science* **1991**, *251*, 1451–1455.
- [4] a) M. Takeichi, *Curr. Opin. Cell Biol.* **1995**, *7*, 619–627; b) S. K. Runswick, M. J. O'Hare, L. Jones, C. H. Streuli, D. R. Garrod, *Nat. Cell Biol.* **2002**, *3*, 823–830.
- [5] a) S. Jothy, S. B. Munro, L. LeDuy, D. McClure, O. W. Blaschuk, *Cancer Metastasis Rev.* **1995**, *14*, 363–376; b) T. Mikami, M. Saegusa, H. Mitomi, N. Yanagisawa, M. Ichinoe, I. Okayasu, *Am. J. Clin. Pathol.* **2001**, *116*, 369–376.
- [6] A.-K. Perl, P. Wilgenbus, U. Dahl, H. Semb, G. Christofori, *Nature* **1998**, *392*, 190–193.
- [7] W. Birchmeier, J. Behrens, *Biochim. Biophys. Acta* **1994**, *1198*, 11–26.
- [8] I. K. Bukholm, J. M. Nesland, R. Karessen, U. Jacobsen, A. L. Borresen-Dale, *Virchows Arch.* **1997**, *431*, 317–321.
- [9] M. Overduin, T. S. Harvey, S. Bagby, K. I. Tong, P. Yau, M. Takeichi, M. Ikura, *Science* **1995**, *267*, 386–389.
- [10] E. Y. Jones, *Curr. Opin. Cell Biol.* **1996**, *8*, 602–608.
- [11] W. Rapp, E. Bayer in *Innovations and Perspectives in Solid Phase Synthesis: Peptides, Polypeptides and Oligonucleotides* (Ed.: R. Epton), Intercept, Andover, **1992**, pp. 259–266.
- [12] O. Seitz, H. Kunz, *J. Org. Chem.* **1997**, *62*, 813–826.
- [13] R. Knorr, A. Trzeciak, W. Bannwarth, D. Gillissen, *Tetrahedron Lett.* **1989**, *30*, 1927–1930.
- [14] a) J. Habermann, H. Kunz, *J. Prakt. Chem.* **1998**, *340*, 233–239; b) J. Habermann, H. Kunz, *Tetrahedron Lett.* **1998**, *39*, 265–268.
- [15] a) H. Matter, G. Gemmecker, H. Kessler, *Int. J. Pept. Protein Res.* **1995**, *45*, 430–440; b) R. Haubner, D. Finsinger, H. Kessler, *Angew. Chem.* **1997**, *109*, 1440–1456; *Angew. Chem. Int. Ed. Engl.* **1997**, *36*, 1374–1389.
- [16] M. Gobbo, L. Biondi, F. Filira, R. Rocchi, T. Piek, *Int. J. Pept. Protein. Res.* **1995**, *45*, 282–289.
- [17] A. Trzeciak, W. Bannwarth, *Tetrahedron Lett.* **1992**, *33*, 4557–4560.
- [18] H. F. Brugghe, H. A. M. Timmermans, L. M. A. van Unen, G. J. Ten Hove, G. van de Werken, J. T. Poolman, P. Hoogerhout, *Int. J. Pept. Protein. Res.* **1994**, *43*, 166–172.
- [19] V. Wittmann, S. Seeberger, *Angew. Chem.* **2000**, *112*, 4508–4512; *Angew. Chem. Int. Ed.* **2000**, *39*, 4348–4352.
- [20] L. A. Carpino, A. El-Faham, *J. Org. Chem.* **1994**, *59*, 695–698.
- [21] **7**: $[\alpha]_D^{25} = -48.2$ ($c = 1.0$, H_2O); MALDI TOF (2,5-dihydroxybenzoic acid, positive-ion mode): m/z : 1371.9 $[M+H]^+$; 1393.8 $[M+Na]^+$; 1H NMR (D_2O , 600 MHz, 1H , 1H -ROESY): $\delta = 8.60$ (s, 1H; Im 2-H), 7.29 (s, 1H; Im 4-H), 4.88 (br s, 1H; Gal 2-H), 3.57–3.54 (m, 2H; Gal 6-H), 2.20–1.96 ppm (m, 11H; Sp, 2 \times E β , 2 \times V β , CH_3CO_2).
- [22] a) P. Boukamp, R. T. Petrussevska, D. Breitkreutz, J. Hornung, A. Markham, N. E. Fusenig, *J. Cell Biol.* **1988**, *106*, 761–771; b) V. M. Schoop, N. Mirancea, N. E. Fusenig, *J. Invest. Dermatol.* **1999**, *112*, 343–353.
- [23] G. Gradl, D. Faust, F. Oesch, R. J. Wieser, *Curr. Biol.* **1995**, *5*, 526–535.
- [24] N. A. Robinson, P. T. LaCelle, R. L. Eckert, *J. Invest. Dermatol.* **1996**, *107*, 101–107.
- [25] a) A. Stöckinger, A. Eger, J. Wolf, H. Beug, R. Foisner, *J. Cell Biol.* **2001**, *154*, 1185–1196; b) I. El-Hariry, M. Pignatelli, N. R. Lemoine, *Int. J. Cancer* **2001**, *94*, 652–661; c) M. A. Perez Moreno, A. Locascio, I. Rodrigo, G. Dhondt, F. Portillo, M. A. Nieto, A. Cano, *J. Biol. Chem.* **2001**, *276*, 27424–27431.

pH-Responsive Molecular Nanocarriers Based on Dendritic Core-Shell Architectures**

Michael Krämer, Jean-François Stumbé, Holger Türk, Simon Krause, Ansgar Komp, Lydie Delineau, Svetlana Prokhorova, Holger Kautz, and Rainer Haag*

Physical aggregates of amphiphilic molecules, such as micellar structures, are frequently proposed as drug-delivery systems.^[1] These aggregates can be unstable under shear force and other kinds of environmental effects as a result of their weak assembly. They are also not very suitable for the active release of the encapsulated species through the application of an external trigger, such as pH change. For drug delivery in biological systems, in particular, the release of the encapsulated species must occur as a result of a weak external signal, for example, a pH drop in tumor and infected tissues (pH 5–6).^[2,3] Furthermore, it has been demonstrated that nanoparticles larger than 5 nm, such as liposomes and macromolecular carriers, can pass through biological membranes by different mechanisms than small molecules, and thereby enhance the specificity of drugs for certain tissues (for example, tumor).^[4–6]

In contrast to physical aggregates of amphiphilic molecules, the covalent modification of dendritic macromolecules^[7] with an appropriate shell results in stable micelle-type structures, which are suitable for the noncovalent encapsulation of guest molecules.^[8] While the encapsulation and the transport of guest molecules into these dendritic architectures have been studied by several research groups,^[9–16] relatively little is known about the active release of the encapsulated guest molecules by the pH-triggered cleavage of the shell under physiological conditions. So far, a pH-dependent release from dendritic architectures has only been reported under drastic conditions^[17] or by protonation of poly(propyleneimine) dendrimers^[18] and their derivatives.^[19,20]

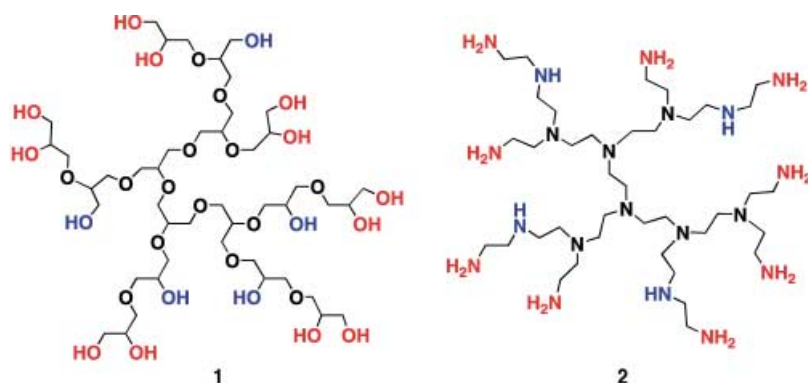
Herein we describe a simple and general synthetic concept for the generation of pH-responsive molecular nanocarriers based on the selective and reversible shell functionalization of dendritic polymers, such as polyglycerol (PG, **1**) and polyethyleneimine (PEI, **2**, Scheme 1). Polyglycerol (**1**) and polyethyleneimine (**2**) are randomly branched, but well-defined dendritic structures with a degree of branching of 60

[*] Dr. R. Haag, Dipl.-Chem. M. Krämer, Dr. J.-F. Stumbé, Dipl.-Chem. H. Türk, S. Krause, A. Komp, Dr. L. Delineau, Dr. S. Prokhorova, Dipl.-Chem. H. Kautz
Freiburger Materialforschungszentrum und
Institut für Makromolekulare Chemie
Universität Freiburg
Stefan-Meier-Strasse 21, 79104 Freiburg (Germany)
Fax: (+49) 761-203-4709
E-mail: rainer.haag@fmf.uni-freiburg.de

[**] The authors would like to thank Prof. Rolf Mülhaupt for his support, and Katrin Armbruster and Bernhard Siegel for the preparation of some intermediates. BASF AG is kindly acknowledged for the donation of chemicals. R.H. is indebted to the Deutsche Forschungsgemeinschaft Fonds der chemischen Industrie and the Dr. Otto-Röhm Gedächtnisstiftung for financial support.



Supporting information for this article is available on the WWW under <http://www.angewandte.org> or from the author.

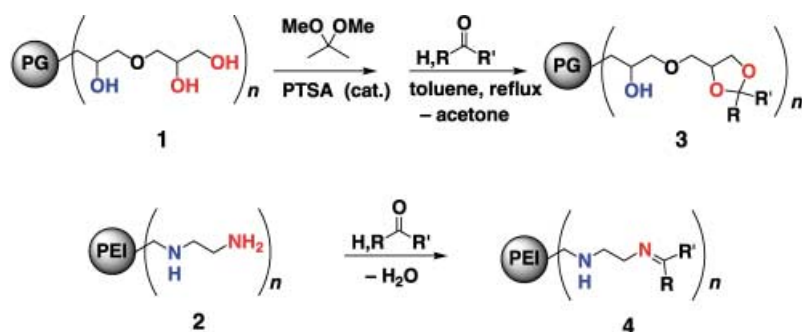


Scheme 1. Polyglycerol (PG, **1**) and polyethyleneimine (PEI, **2**) were used as hydrophilic dendritic core molecules for the selective generation of pH-responsive molecular nano-carriers. The depicted structures containing 30–40% of linear functional groups (blue) and 60–70% terminal groups (red) are only small idealized fragments of the large polymer cores.

to 75%. They are prepared in a one-step process and are readily available on a large scale with low polydispersities (< 2).^[21] The chemical differentiation and selective modification of the linear (blue) and terminal groups (red) in polyglycerol (**1**) results in core-shell-type architectures.^[22] However, a pronounced polarity difference between core and shell is necessary to generate unimolecular micelle-type architectures with good transport properties,^[8] but this was not possible with the previously reported core-shell-type architectures.^[22] We have now developed a general synthetic concept to construct amphiphilic dendritic architectures for potential application in pH-dependent delivery of the encapsulated guest by using two types of acid-sensitive linkages for the shell: PG-acetals/ketals **3** and PEI-imines **4** (Scheme 2).

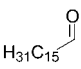
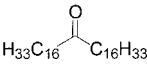
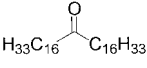
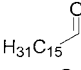
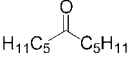
Formally, the selective functionalization of the shell of both dendritic polymers (PG (**1**) and PEI (**2**)) is a simple condensation reaction between the terminal groups (1,2-diol or NH_2 , respectively) and a carbonyl compound. However, the direct conversion of polyglycerol (**1**) with unreactive or lipophilic carbonyl compounds was not possible.^[23] A two-step (one-pot) protocol based on two consecutive transketalization reactions (see Supporting Information) was developed to generate pH-responsive molecular nanocarriers. In the first step PG (**1**) was treated with an excess of acetone dimethyl-acetal to give the corresponding PG-acetonide,^[22] which can subsequently be converted with an equimolar amount of a large variety of carbonyl compounds, for example, long-chain

alkyl ketones, into dendritic core-shell architectures **3**. The situation is even more straight forward in the case of PEI (**2**), since simple nonpolar carbonyl compounds, such as 6-undecanone and 1-hexadecanal, can be directly treated with PEI (**2**) to give the corresponding core-shell architectures **4**.^[24] The reaction even occurs spontaneously at room temperature in the case of hexadecanal. Both types of core-shell architectures (**3** and **4**) are now accessible in high yields (70–90%) and multigram quantities. We have investigated several dendritic core-shell architectures which differ in 1) the type of the core polymer, 2) the molecular weight of the core polymer, 3) the structure of the attached shell, and 4) the density of the attached shell (the degree of alkylation). The transport capacities (amount of encapsulated guest molecules per polymer molecule) of these molecular nano-carriers were first determined using congo red as an easily detectable polar model compound (Table 1). For this purpose the dendritic core-shell architecture was dissolved in chloroform and treated with aqueous dye solutions of different concentrations. Alternatively the guest can also be encapsulated from the solid-phase/organic-solution interface. The amount of encapsulated dye was determined in all cases by UV absorption of the organic phase (see Supporting Information). Similar to other dendritic core-shell architectures,^[8] a minimum core size (ca. 3000 g mol^{-1}) and a highly branched architecture are required for successful encapsulation of the guest molecules.^[14b] For efficient transport the degree of alkylation should be about 45–50% and the alkyl chains should have a minimum length ($> \text{C}_{10}$). For example, the conversion of the terminal groups in polyglycerol **1** (21000 g mol^{-1}) with a C_{16} aldehyde (**3a**) containing one alkyl chain per diol unit results in an effective degree of alkyl functionalization of 25% (Table 1) and a poor transport capacity (0.15 congo red molecules). With the same PG core (21000 g mol^{-1}), the ketal functionalized nanocarrier **3b** with two alkyl chains per diol unit and 45% effective alkyl functionalization (Table 1) can transport up to 13 congo red molecules. A higher degree of ketal functionalization (**3c**: 55%, Table 1) indicates an optimal shell density of 45–50%. However, only two dye molecules were encapsulated in **3c** and the encapsulation process was very slow. Smaller core polymers, shorter alkyl chains, and lower degrees of functionalization also result in lower transport capacities. It is also noteworthy that the selective core-shell architecture **3b** (Table 1) can be up to eight times more efficient than polyglycerols of the same core size randomly functionalized with palmityl ester.^[14a,25] This comparison demonstrates that the polar core environment of these nanocarriers is maximized as a result of the selective core-shell functionalization. The exact determination of the transport capacities for the amine based nanocarriers **4** (Table 1) was complicated because of the hydrolytic sensitivity of the imine-



Scheme 2. General synthetic concept for the generation of amphiphilic core-shell architectures (compare Table 1). Terminal groups (red: 1,2-diols or NH_2 , respectively) were selectively functionalized with aldehydes and ketones by either a twofold transketalization or imine condensation. Linear units (blue) remain unreacted. PTSA = *p*-toluene sulfonic acid.

Table 1. Sizes and transport capacities of dendritic nanocarriers **3** and **4**.

Structure	Polymer core	M_n core [g mol ⁻¹]	Shell	Degree of alkylation	Size ^[a] [nm]	Height ^[a] [nm]	Transport capacity ^[b]
1	PG	21 000	—	—	8 ± 2	2.7 ± 0.6	— ^[c]
3a	PG	21 000		25 %	10 ± 2	2.5 ± 0.5	0.15 ± 0.05
3b	PG	21 000		45 %	10 ± 2	2.7 ± 0.6	13 ± 4
3c	PG	21 000		55 %	10 ± 2	2.5 ± 0.5	2 ± 0.5
2	PEI	25 000	—	—	18 ± 4	3.2 ± 0.5	0.02 ± 0.005 ^[d]
4a	PEI	25 000		33 %	20 ± 4	3.5 ± 0.5	0.6 ± 0.1 ^[d]
4b	PEI	25 000		53 %	84 ± 16	9 ± 2 ^[e]	0.2 ± 0.05 ^[d,e]

[a] Corrected particle diameter and height without encapsulated guest molecules from AFM data (see Supporting Information). [b] Number of encapsulated dye molecules (congo red) per polymeric nanotransporter and transport into the chloroform phase. [c] Not soluble in chloroform. [d] Loading capacities were determined in chloroform without aqueous phase by using a UV calibration curve. [e] Partial hydrolysis and aggregate formation is possible with water.

bound shell in the PEI-based systems in some cases, for example, **4b** (see below). To avoid hydrolysis the dye was directly encapsulated from the solid/organic solution interface. Nevertheless, underestimation might occur because of partial cleavage of the shell.^[26] For comparison, a chemically stable PEI-amide, for example, $M_n(\text{PEI}) = 6000 \text{ g mol}^{-1}$ with a palmitic amide shell (50 %), can encapsulate up to 15 congo red molecules.^[27]

The structure and the particle sizes of these nanocarriers in the unloaded and fully loaded states have been determined with molecular resolution by atomic force microscopy (AFM) in the tapping mode (Table 1, see also Supporting Information). The C₃₃-ketal-functionalized polyglycerol **3b** is shown as an example in Figure 1a. The height of the nanocapsules was obtained from the cross-sectional profiles (for example, recorded along the track marked by the dotted line in Figure 1a) to be in the range of 2–3 nm. The diameter

distribution of the particles was calculated by evaluation of more than 120 particles of each sort and subsequent deconvolution with the AFM tip (Table 1). The number-average diameter of the nanocarrier **3b** appeared to be 10 ± 2 nm for the unloaded state and 13 ± 2 nm for the dye-loaded state (Figure 1b,c). This behavior can be explained by a swelling of the polymer core upon encapsulation of the guest molecules. All the particle sizes determined by AFM studies for the PG-based systems **3** are in good agreement with those calculated by extrapolation from a core with a molecular weight of 4000 g mol⁻¹.^[28] This observation indicates that these dendritic nanocarriers act as inverted unimolecular micelles in dilute solutions (< 10⁻⁴ M). However, larger aggregates are observed at higher concentrations (> 10⁻³ M).^[29] The particle sizes of the PEI-based nanocarriers **4** indicate formation of partial aggregates in some cases as a result of partial hydrolysis on the mica surface (see Supporting Information).^[26] For comparison, the hydrolytically stable PEI-amides, for example, $M_n(\text{PEI}) = 6000 \text{ g mol}^{-1}$ with a palmityl amide shell ($d = 6 \text{ nm}$), show the expected particle sizes.^[27]

The transport properties of these nanocarriers were then tested with different guest structures using the PG- and PEI-based nanocarriers **3** and **4**. Different types of dye molecules containing polar or ionic organic groups were used as model systems. Many organic dyes, such as bromophenol blue, congo red, methyl orange, methyl red, and fluorescein,^[30] all of which contain polar anionic sulfonate or carboxylate groups and sodium counterions, were readily encapsulated and transported by both types of carrier systems **3** and **4** (see also Supporting Information). In contrast, cationic dyes, such as the triphenylmethane-based malachite green with an oxalate counterion, were not transported at all.

The complexation of an antitumor drug (mercaptopurine), several oligonucleotides, as well as bacteriostatic silver compounds (for example, Ag^I salts and Ag⁰ nanoparticles)^[27] have been studied for the potential use of these nanocarriers in drug and gene delivery. Successful encapsulation and transport were observed in all cases by the PEI-based nanocarriers **4**. No complexation, however, was observed with the PG-based nanocarriers **3** for these guest molecules.

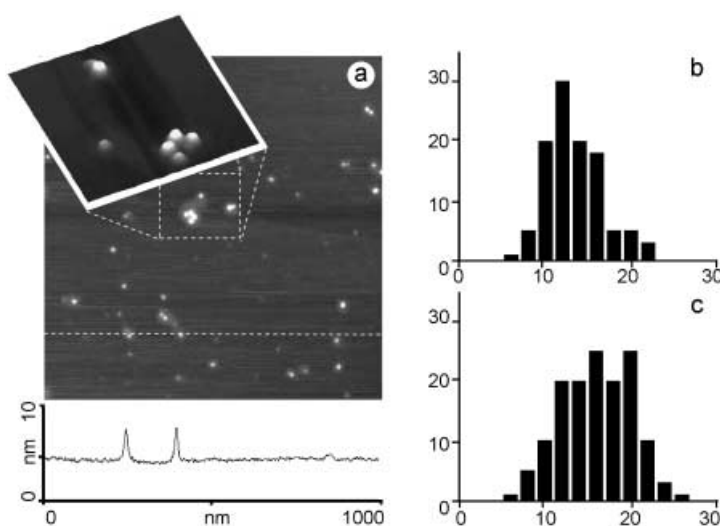


Figure 1. a) AFM images and cross-sectional height profile of individual nanocapsules **3b** prepared by spin-casting of a 10⁻⁵ M solution in chloroform onto a mica substrate. The z-axis scale is 10 nm. The length of the inserted 3D area is 200 nm. Histograms of the size distribution of the: b) unloaded nanocarriers and c) loaded nanocarriers. The histograms were plotted based on the evaluation of more than 120 particles in the AFM images.

The initial objective to develop a pH-sensitive carrier was now tested using several buffer solutions for both the acetal- and imine-bound shells. The encapsulated congo red dye in the nanocarrier **3b** was stable for several months at neutral and basic pH values (pH > 7). However, an immediate release of the guest molecules occurred in acidic media (pH < 3; Figure 2). Since congo red is a pH indicator dye (for pH 4–5), a change of color (red→blue) was observed concurrently with the cleavage of the shell (Figure 2). The cleavage of the PG-ketals also depends significantly on the percentage of shell functionalization: 45 % (**3b**: 2 h, pH 2–3, 37°C) versus 55 % (**3c**: 2 days, pH 0–1, 37°C). The imine-based nanocarriers are even more sensitive to an external drop in the pH value. In the case of nanocarrier **4a** the hydrolysis of the shell and the release of the encapsulated guest (namely, congo red) occurs over a period of four days at pH 6. However, it is stable over several weeks at neutral pH. On the other hand, the hydrolysis of the nanocarrier **4b** and the release of the encapsulated guest even occurs spontaneously at pH < 7. In the case of **4b**, a slow release can be observed after several hours (pH 8, ca. 3 h, 25°C) or days (pH 12, 2 days, 25°C) even without acidification. These PEI-based nanocarriers **4a,b** also show no color change of the indicator dye upon release (Figure 2).

In these release experiments it was demonstrated by dialysis (see Supporting Information) that no complexation of the encapsulated guest (for example, sodium picrate) occurred with either nanocarriers **3** or **4** in the aqueous phase at pH < 7.^[31] For the PEI-based nanocarrier **4b**, the amount of dye release/shell cleavage was followed by IR spectroscopy through the disappearance of the imine signal (Figure 3). The kinetics of the imine hydrolysis on a KBr surface shows a

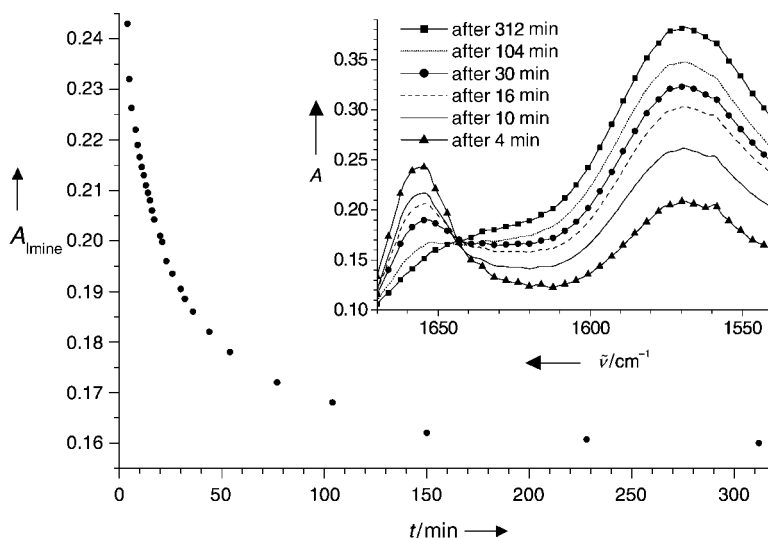


Figure 3. Time-dependence of the shell cleavage of PEI-imine **4b** on a KBr plate. Inset: The IR band of the imine peak at 1655 cm⁻¹ decreases because of cleavage, while the N–H out of plane vibration at 1565 cm⁻¹ increases.

rapid decay over about 3 h. This observation might also explain the formation of aggregates seen by AFM measurements as arising from partial shell cleavage on the mica surface. The analysis of different cleavage stages showed that approximately 30 % shell cleavage is sufficient to destroy the ability of the dendritic macromolecules to act as molecular nanocarriers. This is also supported by the poor transport capacity of a 25 % alkylated core-shell architecture **3a** (Table 1).

Although the detailed mechanism of encapsulation is currently being investigated, the higher selectivity for large anionic guest molecules can be explained by the strong interaction of such species with the polar groups in the core of these dendritic macromolecules. The hydroxy or amine groups in the dendritic core (shown in blue, Scheme 1) can replace the hydrate shell of the polar guest molecules, thus leading to a significant entropic gain by the liberated water molecules. The location of the encapsulated guest molecules (for example, methyl red) inside the dendritic architecture **3b** is also supported by a significant high-field shift (0.2 ppm) of the methyl group signal as a result of the shielding effect of the core-shell architecture, as observed in the ¹H NMR spectrum of the methyl red complex with **3b** (see Supporting Information). In addition, it was not possible to release the encapsulated methyl red from **3b** by either heating to reflux or ultrasonication at neutral pH. This result clearly dem-

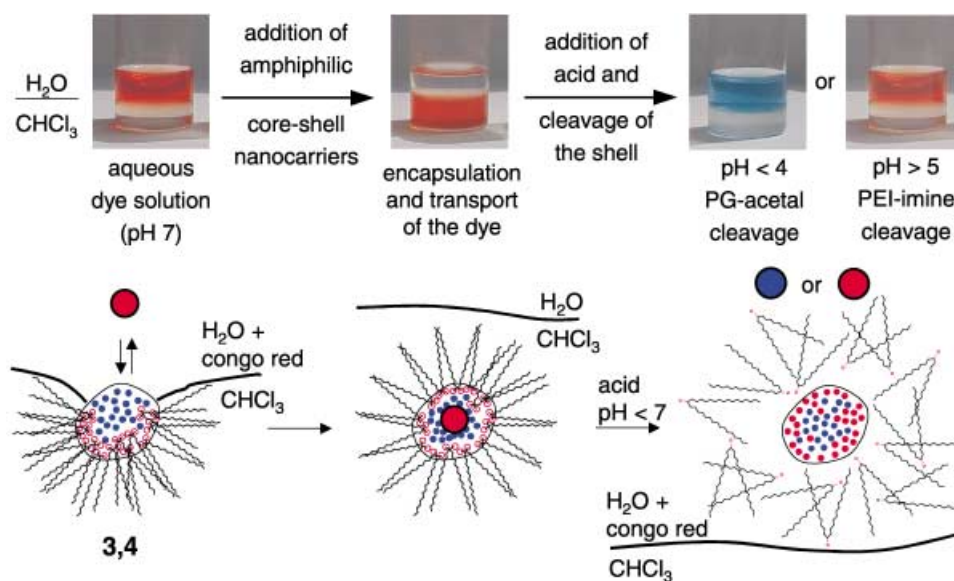


Figure 2. Encapsulation and transportation of polar guest molecules with dendritic nanocarriers **3** and **4** (blue and red dots indicate linear and terminal groups, respectively) into the organic phase. Cleavage of the shell leads to the release of the encapsulated guest back to the aqueous phase. Congo red (pH indicator: pH 4–5) was used as a model compound for the demonstration of the pH-dependent shell cleavage.

onstrates the high mechanical stability of these unimolecular nanocarriers, which is not observed for physical aggregates, such as liposomes or micellar systems. Nevertheless, the release of an encapsulated guest molecule can be achieved by substitution with a molecule of higher binding affinity, as demonstrated by the titration of a bromophenol blue loaded nanocarrier **3b** with a solution of congo red (see Supporting Information). Hence, the encapsulation process is an equilibrium phenomena, which allows the guest molecules to be exchanged by competitive binding. This experiment also indicates that the binding mechanism can not be purely entropically driven and should also contain an enthalpic component.

In summary we have presented a simple general synthetic concept for the selective shell functionalization of dendritic polymers (namely, PG (**1**) and PEI (**2**)) to generate molecular nanocarriers **3** and **4** for the encapsulation and transport of polar guest molecules. The concept is highly flexible in terms of the shell and the core molecules. Dendritic polymers with a pH-responsive shell have been prepared which, for the first time, can selectively release the encapsulated guest molecules in a physiologically relevant pH range. AFM measurements with molecular resolution indicate that these nanocarriers act as inverted unimolecular micelles in concentrations below 10^{-3} M. In addition, various dyes and drugs, for example, bacteriostatic, cytostatic compounds, as well as oligonucleotides have been successfully encapsulated and transported by the amine-based nanocarriers **4**. This concept of pH-responsive molecular nanocarriers might have potential application for selective drug delivery in tissues of a lower pH value (for example, infected or tumor tissue). Further work on the pH sensitivity, biocompatibility, and water solubility of these controlled release systems is in progress.

Received: June 24, 2002 [Z19603]

[1] K. Kataoka, A. Harada, Y. Nagasaki, *Adv. Drug Delivery Rev.* **2001**, 47, 113–131.
 [2] D. E. Hallanan, *Semin. Radiat. Oncol.* **1996**, 6, 243–244.
 [3] P. Vaupel, F. Kallinowski, P. Okunieff, *Cancer Res.* **1989**, 49, 6449–6465.
 [4] H. Maeda, Y. Matsumura, *CRC Crit. Rev. Ther. Drug Carrier Syst.* **1989**, 6, 193–210.
 [5] Y. Takakura, M. Hashida, *Crit. Rev. Oncol. Hematol.* **1994**, 18, 207–231.
 [6] F. Yuan, M. Deilian, D. Fukumura, M. Leuning, D. A. Berk, V. P. Torchilin, R. K. Jain, *Cancer Res.* **1995**, 55, 3752–3756.
 [7] The general term “dendritic” (treelike) structure is used for both hyperbranched polymers as well as perfect dendrimers because of their similar properties with respect to the formation of supramolecular complexes; see also: G. R. Newkome, C. N. Moorefield, F. Vögtle, *Dendritic Molecules: Concepts, Syntheses, Perspectives*, 2nd ed., Wiley-VCH, Weinheim, **2001**.
 [8] M. W. P. L. Baars, E. W. Meijer, *Top. Curr. Chem.* **2000**, 210, 131–182, and references therein.
 [9] G. R. Newkome, C. N. Moorefield, G. R. Baker, M. J. Saunders, S. H. Grossman, *Angew. Chem.* **1991**, 103, 1207–1209; *Angew. Chem. Int. Ed. Engl.* **1991**, 30, 1178–1180.
 [10] J. F. G. A. Jansen, E. M. M. de Brabander-van den Berg, E. W. Meijer, *Science* **1994**, 266, 1226–1229.
 [11] S. Stevelmans, J. C. M. van Hest, J. F. G. A. Jansen, D. A. F. J. van Bortel, E. M. M. de Brabander-van den Berg, E. W. Meijer, *J. Am. Chem. Soc.* **1996**, 118, 7398–7399.

[12] A. P. H. J. Schenning, C. Elissen-Román, J.-W. Weener, M. W. P. L. Baars, S. J. van der Gaast, E. W. Meijer, *J. Am. Chem. Soc.* **1998**, 120, 8199–8208.
 [13] V. Chechik, M. Zhao, R. M. Crooks, *J. Am. Chem. Soc.* **1999**, 121, 4910–4911.
 [14] a) A. Sunder, M. Krämer, R. Hanselmann, R. Mülhaupt, H. Frey, *Angew. Chem.* **1999**, 111, 3758–3761; *Angew. Chem. Int. Ed.* **1999**, 38, 3552–3556; b) S.-E. Stiriba, H. Kautz, H. Frey, *J. Am. Chem. Soc.* **2002**, 124, 9698–9699.
 [15] M. Liu, K. Kono, J. M. J. Fréchet, *J. Controlled Release* **2000**, 65, 121–131.
 [16] C. Kojima, K. Kono, K. Maruyama, T. Takagishi, *Bioconjugate Chem.* **2000**, 11, 910–917.
 [17] J. F. G. A. Jansen, E. W. Meijer, *J. Am. Chem. Soc.* **1995**, 117, 4417–4418.
 [18] G. Pistolis, A. Malliaris, D. Tsiourvas, C. M. Paleos, *Chem. Eur. J.* **1999**, 5, 1440–1444.
 [19] H. Stephan, H. Spies, B. Johannsen, C. Kauffmann, F. Vögtle, *Org. Lett.* **2000**, 2, 2343–2346.
 [20] Z. Sideratou, D. Tsiourvas, C. M. Paleos, *Langmuir* **2000**, 16, 1766–1769.
 [21] For recent reviews, see a) H. Frey, R. Haag in *Encyclopedia of Materials, Science and Technology* (Eds.: K. H. J. Buschow, R. H. Cahn, M. C. Flemings, B. Ilshner, E. J. Kramer, S. Majahan), Elsevier, Oxford, **2001**, pp. 3997–4000; b) H. Frey, R. Haag, *Rev. Mol. Biotechnol.* **2002**, 90, 257–267; c) A. Sunder, R. Mülhaupt, R. Haag, H. Frey, *Adv. Mater.* **2000**, 12, 235–239.
 [22] R. Haag, J.-F. Stumbé, A. Sunder, H. Frey, A. Hebel, *Macromolecules* **2000**, 33, 8158–8166.
 [23] R. Haag, A. Sunder, A. Hebel, S. Roller, *J. Comb. Chem.* **2002**, 4, 112–119.
 [24] The reaction of the symmetrical C₃₃-ketone with PEI (**2**) was not successful according to this procedure.
 [25] For the direct comparison of the transport capacity a polyglycerol palmityl ester (50 % functionalized) was prepared from the same PG core (21 000 g mol⁻¹) according to the procedure published in ref. [14a]: M. Krämer, Diplomarbeit, Universität Freiburg, **2001**.
 [26] A lower degree of alkylation or shorter alkyl chains in **4a,b**, respectively, can result in aggregate formation and hence lower transport capacities.
 [27] R. Haag, M. Krämer, J.-F. Stumbé, S. Krause, A. Komp, S. Prokhorova, *Polym. Prepr. Am. Chem. Soc. Div. Polym. Chem.* **2002**, 43, 328.
 [28] The diameter (*d*) of a PG core with *M_n* = 4000 g mol⁻¹ is about 4 nm according to force-field calculations. Following a mass–volume correlation $M = \rho 4/3\pi(d/2)^3$, the expected radius for a PG core with *M_n* = 21 000 g mol⁻¹ is approximately 8 nm. The diameter of the flexible shell can be estimated to be 1–3 nm.
 [29] Preliminary light-scattering experiments in chloroform gave similar diameters, however, larger aggregates of these particles have been observed at higher concentrations: M. Soddemann, W. Richtering, M. Krämer, R. Haag, unpublished results, **2002**.
 [30] The fluorescence is quenched upon fluorescein encapsulation, which indicates the encapsulated dye molecules are below the Förster distance.
 [31] A salt- and pH-dependent size variation has been reported for amine dendrimers.^[8] However, in the case of compound **4**, this effect should be of minor importance because the terminal amine groups are liberated at the same time as the guest molecules are released.